Materials Today Bio 16 (2022) 100392

Contents lists available at ScienceDirect

Materials Today Bio

journal homepage: www.journals.elsevier.com/materials-today-bio

Catechol-chitosan/polyacrylamide hydrogel wound dressing for regulating local inflammation

Bingyang Lu [a,b], Xiao Han [a,b], Dan Zou [a,b], Xiao Luo [a,b,d], Li Liu [a,b], Jingyue Wang [a,b], Manfred F. Maitz [c], Ping Yang [a,b], Nan Huang [a,b], Ansha Zhao [a,b,*]

[a] Key Laboratory of Advanced Technologies of Materials, Ministry of Education, Southwest Jiaotong University, Chengdu, 610031, China
[b] School of Materials Science and Engineering, Southwest Jiaotong University, Chengdu, 610031, China
[c] Leibniz-Institute of Polymer Research Dresden, Max Bergmann Center of Biomaterials Dresden, Hohe Strasse 6, 01069, Dresden, Germany
[d] School of Medicine, University of Electronic Science and Technology of China, Chengdu, 611731, China

ARTICLE INFO

Keywords:
pH and redox responsive
Resolvin
Drug delivery
Double network hydrogel
Chronic wounds and inflammation

ABSTRACT

Chronic wounds and the accompanying inflammation are ongoing challenges in clinical treatment. They are usually accompanied by low pH and high oxidative stress environments, limiting cell growth and proliferation. Ordinary medical gauze has limited therapeutic effects on chronic wounds, and there is active research to develop new wound dressings. The chitosan hydrogel could be widely used in biomedical science with great biocompatibility, but the low mechanical properties limit its development. This work uses polyacrylamide to prepare double-network (DN) hydrogels based on bioadhesive catechol-chitosan hydrogels. Cystamine and N, N′-Bis(acryloyl)cystamine, which can be cross-linking agents with disulfide bonds to prepare redox-responsive DN hydrogels and pH-responsive nanoparticles (NPs) prepared by acetalized cyclodextrin (ACD) are used to intelligently release drugs against chronic inflammation microenvironments. The addition of catechol groups and ACD-NPs loaded with the Resolvin E1 (RvE1), promotes cell adhesion and regulates the inflammatory response at the wound site. The preparation of the DN hydrogel in this study can be used to treat and regulate the inflammatory microenvironment of chronic wounds accurately. It provides new ideas for using inflammation resolving factor loaded in DN hydrogel of good biocompatibility with enhanced mechanical properties to intelligent regulate the wound inflammation and promote the wound repaired.

1. Introduction

Chronic wounds, such as pressure ulcers, diabetic feet, and venous ulcers of the lower extremities are characterized by various chronic diseases, which usually accompany by continuous chronic inflammatory reactions, not only locate low pH and high oxidative stress environments, but limite cell growth. So, the wound remains in a long-term inflammatory reaction stage and can not remodel or regenerate for tissue repair [1]. Ordinary medical gauze as wound dressing cannot interrupt these inflammatory processes to heal chronic wounds. Multifunctional wound dressings, such as increased granulation tissue formation, vascularization, antibacterial, anti-inflammatory, wound closure et al., are in the focus of development for these cases [2]. Wound repair is facilitated and accelerated in a moist environment [3], suggesting that hydrogels have outstanding potential as wound dressings.

Hydrogels can contain a large amount of water for a long time, some of them also have good biocompatibility and plasticity, especially for natural macromolecular hydrogels, providing them good prospects in many fields of bioengineering, such as tissue engineering and drug carriers [4–6]. Chitosan (CS) is one of the most widely used materials for making hydrogels, and has been considered for wound dressing applications, with its excellent biocompatibility, low toxicity and immune-stimulatory activities [7,8]. Due to these properties, chitosan shows good biocompatibility and positive effects on wound healing. It can also accelerate repair of different tissues and facilitate contraction of wounds [9]. However, CS hydrogels without cross-linking agent have a dense scale-mesh like network which only allow for passive diffusion nutrients and metabolic wastes being not suitable for biomedical applications [10]. Furthermore, it has a weak mechanical properties and uncontrolled dissolution [11,12]. The advent of double network hydrogels

* Corresponding author. Key Lab. for Advanced Technologies of Materials, Ministry of Education, School of Material Science and Engineering, Southwest Jiaotong University, Chengdu, 610031, China.
E-mail address: anshazhao@263.net (A. Zhao).

https://doi.org/10.1016/j.mtbio.2022.100392
Received 19 May 2022; Received in revised form 1 August 2022; Accepted 2 August 2022
Available online 11 August 2022

is a solution, as it enhances the mechanical properties of natural hydrogels while maintaining the biocompatibility [13,14].

Hydrogels wound dressings need to have various functions for achieving better repaired. Catechol groups, discovered as adhesive molecules of marine mussels [15,16], also can provide tissue adhesion and healing properties to hydrogels [17–20]. Gan et al. prepared a mussel-inspired hydrogel that promoted wound healing, and enhanced the antibacterial property of the hydrogel to prevent wound infection through the quaternization of the side chain [21]. Gan et al. also used catechol groups to modify Ag-lignin NPs and used these NPs to enhance the toughness and adhesion of the hydrogel through covalent and non-covalent interactions in the hydrogel network formed by polyacrylic acid and pectin [22]. In short, the use of catechol groups to modify hydrogel wound dressings promotes the adhesion of the hydrogel to tissues and cells that promotes wound healing.

Hydrogels can serve as drug delivery systems with therapeutic and regulatory effects [23]. An intelligent release of the drug can increase its bioavailability and improve the therapeutic effect in the lesion environment [24–27]. Responsive groups such as disulfide bonds [28,29], acetal groups [30,31], or others can provide responsiveness to Reactive oxygen species (ROS), pH, or others. However, due to the highly hydrated nature of hydrogels, they are suitable for releasing hydrophilic drugs. In contrast, hydrophobic drugs are difficult to disperse in the hydrogel, limiting the development of hydrogel drug delivery systems in such cases. Small drug molecules are released rapidly diffusion controlled from the hydrogel structure, what makes controlled release difficult [25]. Growth factors, curcumin and other drugs have been suggested for the release from hydrogels as wound dressings, which could anti-inflammatory, cell growth regulation et al., with a synergistic effect on the hydrogel to promote wound healing [32,33]. However, chronic wounds remain in the inflammatory phase for a long time during the recovery process, it require regulation of the inflammatory situation and promotion of the repair-type inflammation, and the macrophages play a key role to regulate it, especially the M_2 phenotype release the anti-inflammatory factors such as IL-4 and IL-10 [34,35]. The inflammatory influence the microenvironment to low pH and high ROS. There are a few studies on wound dressings in anti-inflammatory/promoting regeneration. Specialized pro-resolving lipid mediators (SPMs), such as RvE1, Resolvin D1 (RvD1) et al., are endogenous polyunsaturated fatty acid derivatives that influence macrophages and other cells for inflammation regression and tissue repair [36]. SPMs influence the transformation of the macrophage phenotypeare through leukotriene ratio changed, are the most promising endogenous anti-inflammatory drugs with high activity and low dose [37,38].

In this study, a ROS-responsive hydrogel is formed using catechol-chitosan (C-CS) with Cys cross-linking, and the polyacrylamide (PAM) was cross-linked by Bis(acryloyl)cystamine (BAC) and N, N' -Methylene-bis-(acrylamide) (MBA), which were used to prepare a DN hydrogel named C-CS/PAM-MBA, C-CS/PAM-BAC, C-CS-Cys/PAM-MBA, C-CS-Cys/PAM-BAC, respectively. The β-cyclodextrin (β-CD) was acetalized modified and formed NPs through self-assembly, which loaded the ACD-NPs to respond to the low pH and high ROS caused by inflammation in chronic wounds, respectively [39,40]. After loading RvE1 on ACD-NPs, the drug-loaded particles were loaded into the double-network hydrogel to prepare a hydrogel drug-delivery system, and this hydrogel drug-delivery system was used for the treatment of chronic wounds, as shown in Fig. 1. This provided a new idea for the hydrogel wound dressing to intelligently regulate the inflammation of hard-to-heal wounds and promote wound healing.

2. Experimental section

2.1. Materials

Chitosan (CS, 100–200 mPa.s, more than 95% degree of deacetylation), 3,4-Dihydroxyhydrocinnamic acid (DHPA, 98%), 1,4-Dithiothreitol (DTT, ≥ 97%), N, N' -Methylene-bis-(acrylamide) (MBA, 99%), Cystamine Dihydrochloride (Cys, > 97.0%) were purchased from Shanghai Aladdin Biochemical Technology Co., Ltd (Shanghai, China). Phenyl (2,4,6-trimethylbenzoyl) phosphate lithium salt) (Photoinitiator LAP, > 97.0%), 2-Methoxyproene (MP, 98.0%), Pyridinium p-toluenesulfonate (PTS, 98.0%), N-(3-Dimethylaminopropyl)-N′-ethylcarbodiimide hydrochloride (EDC, ≥ 98%), β-Cyclodextrin (β-CD, ≥ 97.0%), Dopamine Hydrochloride (DOPA) were purchased from Sigma-Aldrich (U.S.A.). Acrylamide (AM), N, N′-Bis(acryloyl)cystamine (BAC, 98%), Triethylamine (99.0%) were purchased from Shanghai Macklin Biochemical Co., Ltd (Shanghai, China). Dimethyl sulfoxide (DMSO, 99.7%) were purchased from Shanghai Macklin Biochemical Co., Ltd (Shanghai, China). Resolvin E1 (RvE1, ≥95.0%) was purchased from Cayman Chemical (U.S.A.). Trypsin (0.25%), Penicillin, Streptomycin, DMEM (Dulbecco's Modified Eagle Medium) Basic medium, DMEM F12 medium, DMEM High Glucose medium, Bovine serum albumin (BSA),

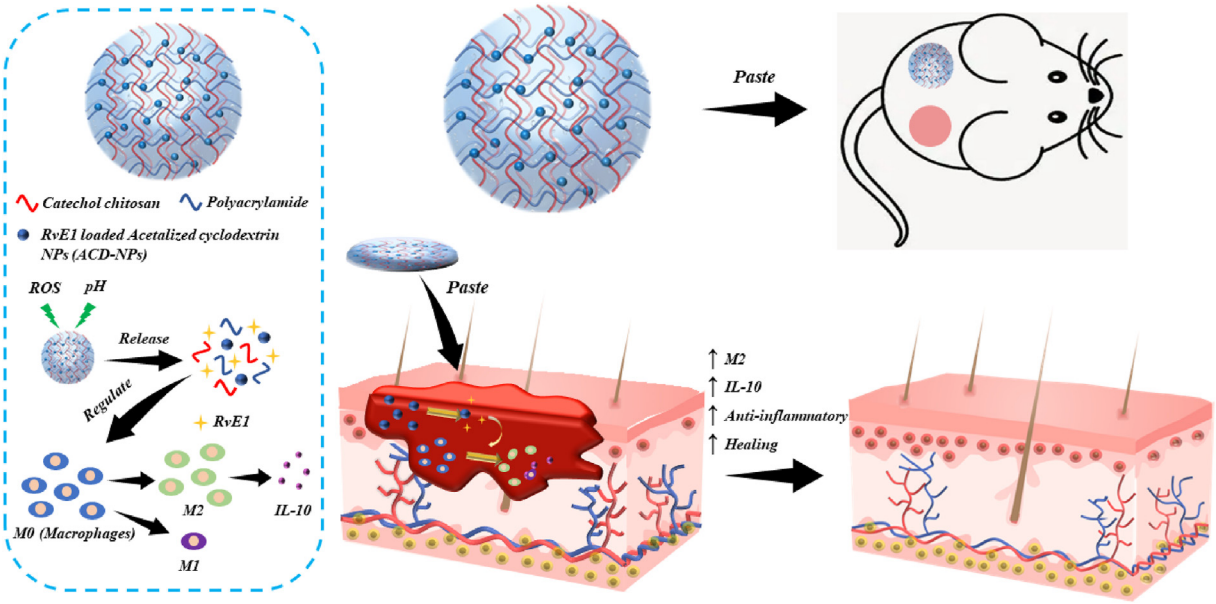

Fig. 1. DN hydrogel responsively released RvE1 to promote wound healing.

etc., were all purchased from Wuhan Saiweier Biotechnology Co., Ltd (Wuhan, China).

2.2. Preparation and characterization of the C-CS

The modification process of catechol-chitosan has been reported in previous work [41]. Briefly, the CS was dissolved in RO water (pH = 4-6), and the DHPA was grafted to the CS by carbodiimide chemistry. After dialyzing and freeze-drying, the C-CS was prepared successfully. The UV spectrum was recorded with a TU-1901 spectrometer (Shenzhen Yixin Instrument Equipment Co., Ltd). The Proton Nuclear Magnetic Resonance Spectrum (^{1}H NMR, 400 MHz) was tested with a Varianunity Inova-400 Spectrometer (American Varian Company). By changing the feed ratio of the catalyst EDC and the monomer DHPA in the chitosan modification formula, a series of chitosan with different grafting rates was obtained. The formula and grafting rates were shown in Table S2.

2.3. Preparation and characterization of the C-CS and the C-CS-Cys hydrogels

C-CS was placed in Tris-base solution (pH = 8.5) and completely dissolved in an ice bath while stirring. Then Cys solution in Tris-base was added slowly to the C-CS solution and the solution was kept stirring for about 2 h to oxidize the catechol groups. The mixture solution was stirred vigorously for 5 min at controlled temperature (37 °C) for gelation to prepare the C-CS-Cys hydrogel. The C-CS hydrogel was prepared in the same way without the addition of Cys. C-CS with different grafting ratios were used to prepare modifications of the hydrogel. This work used different feed ratios to gain the catechol-chitosan with different grafting rates (as in Table S2). The different preparation conditions, explored for the formation of the C-CS and C-CS-Cys hydrogels, are in Table S3.

After freeze-drying, the C-CS and C-CS-Cys hydrogels were characterized by FT-IR and XPS using a Nicolet-5700 Fourier Infrared Spectrometer and a PHI-5400 Perkin Elmer X-ray photoelectron spectrometer, respectively. C-CS-Tris sample was re-dried after dissolution in Tris-base solution.

2.4. Preparation of the DN hydrogel

The 20% Acrylamide (AM), 0.2% photoinitiator Phenyl (2,4,6-trimethylbenzoyl) phosphate lithium salt (LAP) and crosslinking agent (0.2% N, N′-Bis(acryloyl)cystamine (BAC) or 0.12% N, N' -Methylene-bis-(acrylamide) (MBA) were well mixed in PBS. And then the C-CS hydrogel and C-CS-Cys hydrogel were immersed into the mixed liquids, respectively, until equilibration (enough time about 24 h). After UV irradiation (1 min, 2 mW/cm^2) to initiate free radical polymerization, the DN hydrogel was prepared. The DN hydrogels were characterized by XPS to analyze the form of sulfur.

2.5. Preparation of the ACD-NPs

Preparation of the ACD-NPs: the synthesis process of ACD was according to Zhang's work [42]. In short, 2-methoxyproene (MP) was grafted onto β-cyclodextrin (β-CD) with pyridinium *p*-toluenesulfonate (PTS) as catalyst and triethylamine as terminator in anhydrous DMSO; the chemical reaction equation is shown in Fig. S9. ACD was dissolved in 500 μL acetonitrile (10 mg/mL), which was dropped to 4 mL Reverses Osmosis (RO) water at 1 droplet per minute to self-assemble NPs in 40 kHz ultrasound. After 5 min centrifugation at 12,000 r/min and washing by RO water, the ACD-NPs were successfully prepared.

2.6. Preparation of the RvE1 loaded C-CS-Cys/PAM-BAC hydrogel

Ethanol was used to dissolved RvE1 to 5 μg/mL, and 0, 40, 80, 120 μL of this stock solution were mixed with ACD dissolved in acetonitrile. Then, the different loaded RvE1-ACD-NPs were self-assembled after centrifugation and dispersion in RO water. The DN hydrogel was immersed in RO water to remove the AM, and the 1 mg/mL RvE1-ACD-NPs were completely absorbed by the dry DN hydrogel, which had prepared DN hydrogel loaded the 40, 80, 120 ng/mL RvE1.

2.7. Test of swelling and mechanical properties

The tensile and compression properties of DN hydrogel were tested by a universal testing machine (Instron 5575, USA). The samples for compression testing were cylinders with 8 mm height and 10 mm diameter. The samples for tensile testing were cuboids with 8 mm height and 3 mm diameter.

The freeze-dried DN hydrogel was immersed in PBS, measuring the weight and volume at 0, 0.5, 1, 3, 6, 12, 24, 36, 48, 72 h, and calculating the volume swelling rate (λ_v) and weight swelling rate (λ_w) with equations 1, and 2, respectively. W_i was the weight of the samples after swelling, while the W_0 was the initial weight of the samples. H_i and D_i were the height and diameter of bottom surface after swelling, while the H_0 and D_0 were the initial height and diameter of the bottom surface.

$$\lambda(w) = \frac{W_i}{W_0} \tag{1}$$

$$\lambda(\nu) = \frac{\pi \times \left(\frac{D_i}{2}\right)^2 \times H_i}{\pi \times \left(\frac{D_o}{2}\right)^2 \times H_o} \tag{2}$$

2.8. Responsive of hydrogel and drug release

PBS (1 mL) with or without 5% H_2O_2 were added to the C-CS-Cys hydrogel (Gelled by 1 mL RO water). The glass bottle with the hydrogel were put in 37 °C with shaking every 4 h for improved contact with H_2O_2. After 3 and 6 days, the C-CS-Cys hydrogel in PBS with H_2O_2 was gradually became liquid.

The ACD-NPs-RvD1 loaded C-CS-Cys/PAM-BAC hydrogel was placed into 1 mL of PBS at pH = 5.4 or pH = 7.4, another sample was placed into 1 mL of PBS at pH = 5.4 with 2 mM H_2O_2, incubated at 37 °C, 100 μL of release medium was withdrawn at 6, 12, 24, 72, 120 h, and the same volume of corresponding fresh medium was replenished. The RvD1 release was quantitatively determined by ELISA (Cayman Chemical, USA). RvD1 has similar characteristics as RvE1, when the trace amounts of RvE1 have not had a great way to measure.

2.9. In vitro growth of cells on the RvE1 loaded C-CS-Cys/PAM-BAC hydrogel

In vitro growth of cells on the RvE1 loaded C-CS-Cys/PAM-BAC hydrogel: C-CS-Cys/PAM-BAC hydrogels loaded with different concentrations of RvE1 were spread in a 24-well plate. Macrophages (RAW 264.7), and L929 fibroblasts were cultured on the RvE1 loaded C-CS-Cys/PAM-BAC hydrogel. The viability of the cells was tested by Cell-Counting-Kit-8 (CCK-8) assay, and the proliferation was observed by fluorescence microscopy after Acridine Orange (AO) staining. The macrophage medium was used to test the inflammatory factors (TNF-α and IL-10) with ELISA. The macrophage chemotaxis was tested with transwell. Details were described in the Supporting Information.

2.10. The test of RvE1 loaded C-CS-Cys/PAM-BAC hydrogel for wound dressing in vivo

All procedures were performed in accordance with the Animal Protection Agreement of the China Animal Protection Association and Southwest Jiaotong University, and all ethical guidelines for experimental animals were followed. SD rats (Female, 7 weeks, about 180 g) were purchased by Ensiweier Chengdu Co, Ltd. After adapting to the living environment, full-thickness skin wounds were created on the back

of SD rats by hole punch (d = 8 mm). C-CS-Cys/PAM-BAC hydrogels loaded with different concentrations of RvE1 or PBS were put into the wounds. The wound repair was observed through HE and Masson staining until wound healing at 20 days. Every samples were repeated and put into the wounds for 5 rats.

2.11. Statistical analysis

All experiments were performed at least three times, and the results are expressed as mean ± standard deviation (SD). One-way analysis of variance (ANOVA) was used to analyze the experimental results, and the statistical difference between two groups was considered significant when $p < 0.05$.

3. Results

3.1. The synthesis of C-CS and the preparation of C-CS and C-CS-Cys hydrogels

The dopamine (DOPA) was grafted onto the CS with the formation of amide bond. The C-CS was characterized by ultraviolet (UV), which showed the characteristic peak of the catechol group at 280 nm, confinming DOPA, which was absent in CS as shown in Fig. 2(a). It can be seen that the catechol-modified chitosan and dopamine had a strong characteristic absorption peak at 280 nm, while native chitosan had no absorption peak at 280 nm [43]. This indicates that DHPA was successfully grafted onto chitosan. The C-CS was also analyzed by ^{1}H NMR (Fig. 2(b)). The peak at 4.79 ppm was characteristic for the solvent heavy water (D_2O), the peak at 3.1 ppm belonged to C-2 of the chitosan sugar ring, the peak at about 2.1 ppm belonged to the acetylated methyl group (-O═CH_3), and the peak between 6.60 and 6.88 ppm belonged to the characteristic peak of the hydrogen proton on the benzene ring. Zhang et al. [44] carried out a similar characteristic peak analysis, and it was shown that the unmodified chitosan had no characteristic peak at 6.60–6.88 ppm. From the ratio of the peak area integration of a single hydrogen proton on the benzene ring to the peak area integration of the only hydrogen proton on C-2 in the chitosan backbone, the ratio of the number of moles of hydrogen atoms between the two can be obtained, which was the grafting rate of C-CS. The grafting rate of C-CS this way was determined as 12.3 ± 0.5%, and the deacetylation rate was about 96% (> 95%). The grafting rates of C-CS with different feeding ratios were calculated as showed in Table S2. Cys added to the C-CS solution as a cross-linking agent accelerated the formation of the hydrogel (Fig. 2(c)).

The C-CS-Cys hydrogel did gelate at only 1 day, whereas the C-CS hydrogel needed approximately 5–7 days for gelation. The C-CS hydrogel expressed a pink color (Fig. 2(c)). The gelation times of using different gelling processes was shown in Table S3 and Fig. S1, the Fig. S1 (a-d, f) were not being hydrogel, but the hydrogel in Group g was most uniform. The C-CS-Cys hydrogel formed at 37 °C with 1% catechol-chitosan at the grafting rate of 12.3 ± 0.5% and Cys concentration of 8% had the best gelation, as shown in Fig. S1(g). A C-CS hydrogel formed in same condition without Cys served as control group (Fig. S1(l)).

3.2. Structure and performance characterization of the C-CS and C-CS-Cys hydrogels

The C-CS and C-CS-Cys hydrogels were analyzed by FT-IR (Fig. 2(d)) and XPS (Table 1) and (Fig. 2(e–h)) to test the structure composition and cross-linking mode. The FT-IR showed a peak at about 3419 cm^{-1}, characteristic for the stretching vibration peak of –OH, and the strong peak at 1625 cm^{-1}, indicating the stretching vibration peak of C═O. The stretching vibration peak of aromatic C═C appeared at about 1550 cm^{-1}, and the peak at 1075 cm^{-1} was the typical stretching vibration peak of C–O in CS [41]. The spectra of C-CS, C-CS-Tris (C-CS dissolved in

Table 1
Element content of C-CS and C-CS-Cys hydrogels.

Sample	C (%)	N (%)	O (%)	S (%)
C-CS	65.57	7.17	25.39	1.88
C-CS-Cys	65.03	6.36	26.49	2.13

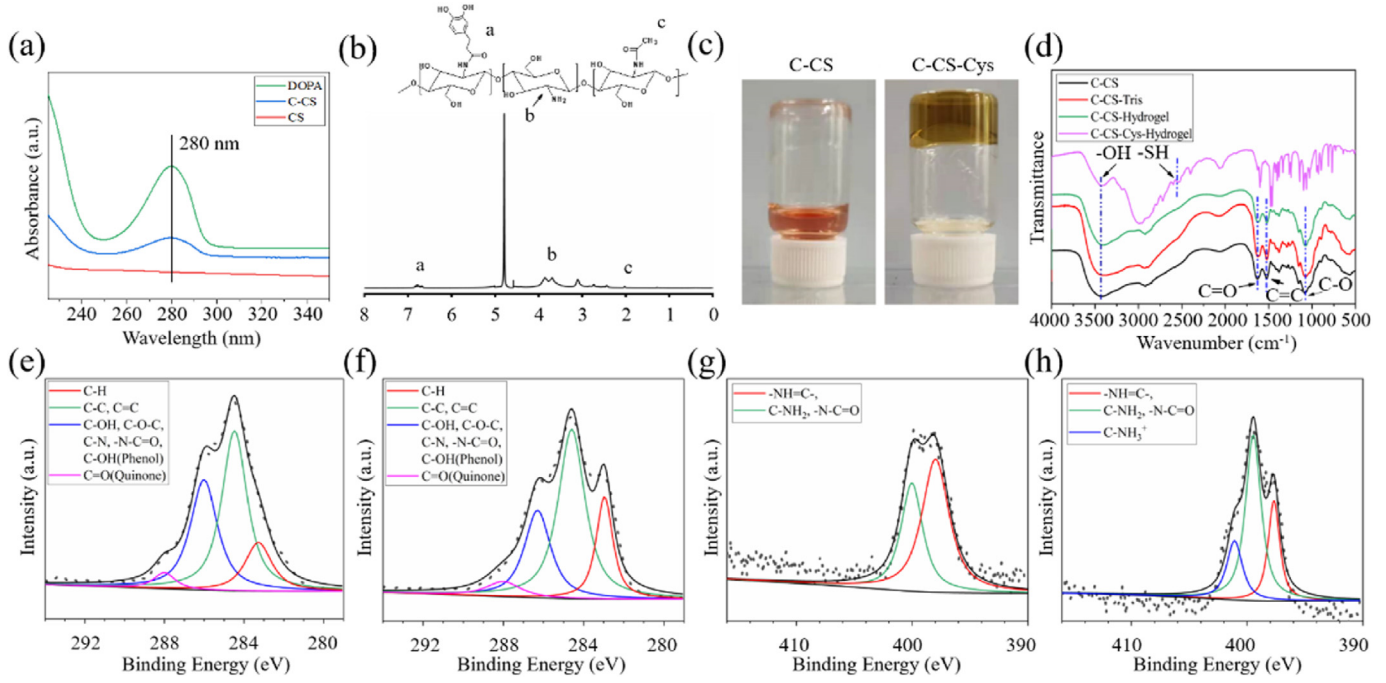

Fig. 2. (a) UV absorption spectra of CS, C-CS, and DOPA. (b) ^{1}H NMR spectrum of C-CS in D_2O. (c) Gelation of C-CS and C-CS-Cys hydrogel at 1 day. (d) Infrared absorption spectrum of C-CS, C-CS-tris, C-CS hydrogel, and C-CS-Cys hydrogel. XPS high resolution (e) C spectrum (g) N spectrum of C-CS, and XPS high resolution (f) C spectrum (h) N spectrum of C-CS-Cys hydrogel.

Tris-base suffer solution and freeze-drying), and C-CS hydrogel were basically the same, indicating that C-CS hydrogel were only physically and not chemically cross-linked. In the C-CS-Cys hydrogel peaks of figure 2(d), a vibration peak of –SH was found at about 2500 cm^{-1}, which preliminarily proved the formation of a cross-linked network of Cys, but during the gelation process, the unstable disulfide bonds were partially reduced to –SH.

The element content of the C-CS and C-CS-Cys hydrogels was determined by XPS. Sulfur of C-CS hydrogel was 1.88%, and increased to 2.13% for the C-CS-Cys hydrogel. The two hydrogels' high-resolution spectra of C and N elements showed split peaks. The peak of the high-resolution C spectrum at about 288.0 eV showed oxidation of the catechol group to benzoquinone in the weakly alkaline tris-base solution during the gelation process. The new peak of the high-resolution N spectrum at about 401.1 eV was due to the formation of $C–NH_3^+$, which indicated that the Michael addition reaction had undergone between amino group of Cys and the catechol group, so that Cys was integrated in the network structure of the hydrogel as a crosslinking agent, and accelerates the cross-linking time of the C-CS-Cys hydrogel.

3.3. Swelling performance of the DN hydrogels

The volume and mass swelling curves of the freeze-dried DN hydrogel in PBS were shown in Fig. 3(a) and (b). And the changed condition of the DN hydrogels before and after swelling as shown in Fig. 3(c), the DN hydrogels had obviously changed in topography. In the first 12 h, the swelling speed of the DN hydrogels was fast, and the swelling reached an equilibrium after 36 h. The pure C-CS and C-CS-Cys hydrogels, swelled only in the first 0.5 h and then reached the equilibrium. Compared with the chitosan single-network hydrogel prepared, the volume swelling rate of the DN hydrogels increased from 4.06 (C-CS) and 8.18 (C-CS-Cys) to 23.38–32.40, and the mass swelling rate increased from 4.07 (C-CS) and 1.96 (C-CS-Cys) to 9.29–12.48.

The DN hydrogels obviously had better swelling properties, allowing them to absorb more liquid. One reason might be the better swelling properties of PAM used as the second hydrogel network, which caused by high hydrophilicity of PAM compared with CS.

3.4. Mechanical properties of the DN hydrogels

The purpose of preparing DN hydrogels was to enhance the mechanical properties of the chitosan hydrogel, as shown in Fig. 3. The tensile strengths of the C-CS and C-CS-Cys hydrogels were 0.006–0.007 MPa, while the tensile strengths of the DN hydrogels were all above 0.030 MPa. And the tensile strength of C-CS-Cys/PAM-BAC hydrogel was the highest, reaching 0.126 MPa, which preliminarily showed that the double network improved the tensile strength of the hydrogel. At the same time, the C-CS-Cys/PAM-BAC hydrogel can reach 3 times the length

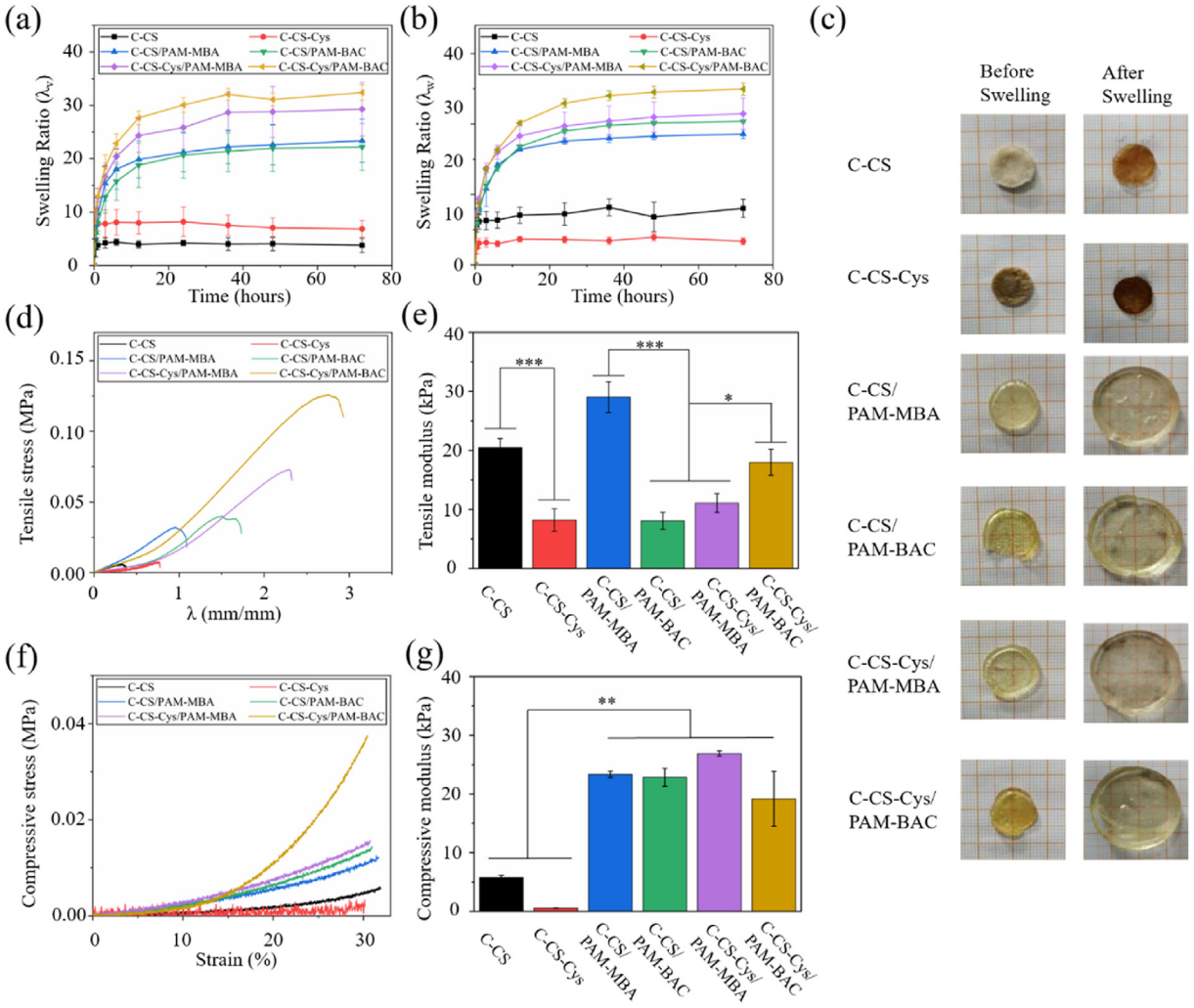

Fig. 3. (a) Volume swelling curve and (b) mass swelling curve of double network hydrogels. (c) Photo of hydrogel before and after swelling. (d) Tensile stress-strain curve, and (e) tensile modulus of DN hydrogel. (f) Compressive stress-strain curve, and (g) compressive modulus of DN hydrogel. (n = 3, *p < 0.05, **p < 0.01, ***p < 0.001).

of the original level during the stretching process, which indicated that the ductility of DN hydrogels also greatly improved. The tensile modulus of C-CS hydrogel was higher than that of C-CS-Cys hydrogel because the addition of cystamine caused more rapid formation of the hydrogel, but also more defects. The tensile modulus of C-CS/PAM-MBA was the highest, reaching 28.2 kPa, which indicated that the DN hydrogels prepared by this way had the best stability. The tensile modulus of C-CS/PAM-BAC and C-CS-Cys/PAM-MBA hydrogels were significantly lower, which may be related to the addition of disulfide bonds, and the chain length of BAC was longer than MBA so that the degree of cross-linking was decreased. The tensile modulus of the C-CS-Cys/PAM-BAC hydrogel prepared after adding disulfide bonds in both two networks had increased on the contrary, which may be related to the dynamic interaction between the disulfide bonds in the two hydrogel networks [45,46].

As shown in Fig. 3 (f), the compressive strength of the four DN hydrogels were significantly higher compared to the single-network hydrogels, with the highest values for the C-CS-Cys/PAM-BAC hydrogel. Fig. 3 (g) showed the compressive modulus. The compressive modulus of the DN hydrogels was also significantly higher than that of the single-network hydrogel, from below 5 kPa to a maximum of about 27 kPa. The reason was similar to that of the change in tensile properties.

3.5. The properties of the DN hydrogels

The hydrogels were observed by SEM at 100 × magnification, as shown in Fig. 4(a–f). The pore size in the C-CS hydrogel was about 100–200 μm, while the surface of the C-CS-Cys hydrogel did not have an obvious network structure. The DN hydrogels all had pores with sizes in the range of 10–20 μm, which were significantly smaller than C-CS and C-CS-Cys hydrogels.

The S content in the hydrogel was determined by XPS, the high-resolution spectra of S were shown in Fig. 4(g–l). The peak at 168.68 eV represented the group of RSS(O)R, and the peak at 163.98 eV indicated the appearance of RSSR and RSH. The peaks of RSSR and RSH in the C-CS-Cys hydrogels were significantly increased, compared with C-CS hydrogel, which had no peak in the high-resolution spectrum of S.

According to the analysis of the peak areas, there were almost no disulfide bond peaks in the C-CS/PAM-MBA hydrogel, whereas 20.0% RSSR and RSH groups appeared in the C-CS/PAM-BAC hydrogel due to the disulfide bond in the cross-linking agent N, N′-Bis(acryloyl)cystamine (BAC) used in the second layer polyacrylamide hydrogel network. In the C-CS-Cys/PAM-MBA hydrogel, the area of the peak of the RSSR and RSH groups was 11.7%, which was caused by the disulfide bonds formed by

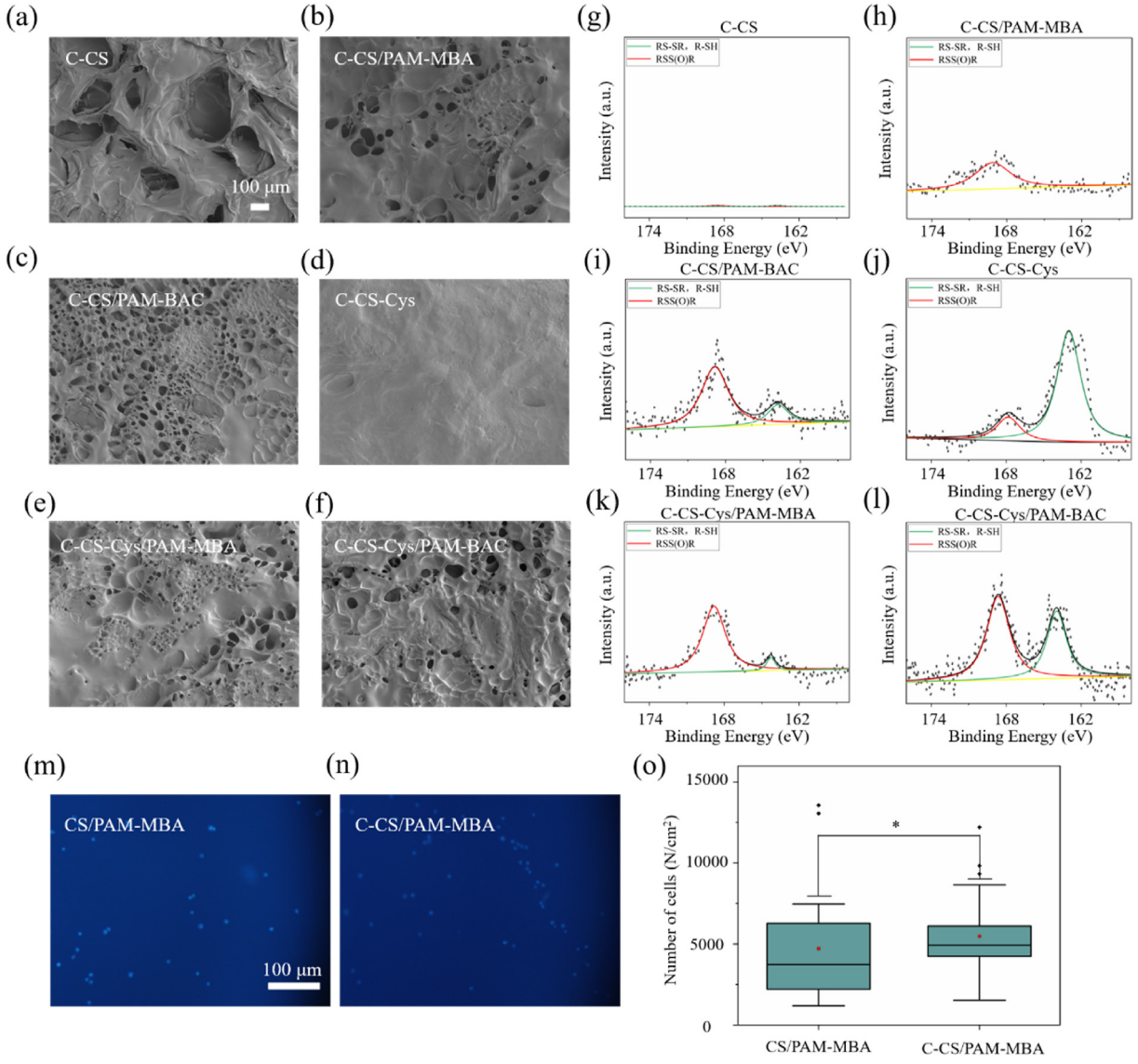

Fig. 4. (a–f) SEM images of the different hydrogel samples. (g–l) XPS high resolution S spectra of different hydrogel samples. (m–n) DAPI staining of fluorescent image of EC adhesion on the hydrogel. (o) Box plot of EC adhesion on the hydrogel. (n = 9, Pic = 36, *p < 0.05).

the crosslinking agent Cys in the C-CS-Cys hydrogel. In the C-CS-Cys/PAM-BAC hydrogel, the peak area of RSSR and RSH groups was 39.3%, due to the dynamic reaction of the disulfide bonds increased the stability between BAC and Cys, and the more additional disulfide bonds in the C-CS-Cys/PAM-BAC hydrogel. Therefore, there were many and stable disulfide bonds in the C-CS-Cys/PAM-BAC hydrogel system.

The Fig. 4 (m,n) showed the adhesion of Endothelial cell (EC) on the hydrogel after 12 h, after staining with 4′,6-diamidino-2-phenylindole (DAPI). The numerical evaluation was shown in Fig. 4 (o), the ECs tended to stick on the C-CS/PAM-MBA hydrogel compared with CS/PAM-MBA, which indicated that the catechol group in hydrogel promoted the adhesion of cells. The abnormal points in Fig. 4 (o) might be caused by the uneven surface of hydrogel after swelling in cell culture medium.

3.6. Characterization of the ACD-NPs

In order to control the drug release behavior of DN hydrogels, ACD-NPs were designed to load drugs and added to the DN hydrogel. The chemical reaction equation of acetalized modified cyclodextrin was shown in Fig. S2, and the results of FT-IR and ^{1}H NMR of the ACD were shown in Figs. S3 and S4. The FT-IR showed a blue shift of the –OH stretching vibration peak (3390 → 3469 cm^{-1}) Because the methoxy was the electricity-absorbing group, and the hydroxyl absorption peak was significantly reduced after grafting the acetal group. The peaks at 2993, 2940, and 2834 cm^{-1} were the stretching vibration peaks of the C–H of the methoxy group on the linear acetal, and the absorption peak at 1457 and 1375 cm^{-1}, and at 1216, 1157, 875, and 848 cm^{-1} were obvious deformation vibrations of C–H absorption and skeleton C–C vibration absorption peaks of the acetal group C(CH$_3$)$_2$, respectively.

The ^{1}H NMR showed the peak at 2.5 ppm corresponding to DMSO-d_6, and the peak at 3.3 ppm corresponding to DOH. The H peak of C-1 was at 4.83 ppm, and the H of the three –OH groups were at 4.48, 5.71, 5.75 ppm, as shown in Fig. S4 (a). The new peaks at 1.3–1.5 ppm were caused by the β-CD modifying with (CH$_3$)$_2$C═, and the peaks at 3.05–3.08 ppm were formed by CH$_3$ at the acetal, as shown in Fig. S4 (b). The degree of acetalization of the cyclodextrin was 77.6%, calculated from the peak area. The results of FT-IR and ^{1}H NMR showed that the ACD was successfully modified [42,47].

After self-assembly of the ACD-NPs, they had sizes of 70 nm and 300 nm, as observed by TEM (Fig. S5), which might be caused by linear versus cyclic acetalization to β-CD. Tested by dynamic light scattering, the particle size of the ACD-NPs was 607.1 ± 8.2 nm but increased to 681.4 ± 11.2 nm after 6 h of incubation in PBS with pH = 5.4. After loading with 0.2 μg/mL of RvE1 with pH = 7.4, the particle size increased to 652.2 ± 6.1 nm, and after incubation in PBS with pH = 5.4 for 6 h, the particle size of the RvE1 loaded NPs (ACD-NPs-RvE1) increased to 891.1 ± 15.6 nm (Table S4 and Fig. S6). This demonstrated that the inflammatory regulatory factor RvE1 was successfully loaded into ACD-NPs, and ACD-NPs had pH responsiveness.

3.7. ROS response of C-CS-Cys hydrogels and drug release of C-CS-Cys/PAM-BAC hydrogels

The C-CS-Cys hydrogels were immersed into PBS with or without 5% H_2O_2, as shown in Fig. 5 (a). The hydrogel structure added with 5% H_2O_2 solution was almost completely destroyed after 6 days when the hydrogel without 5% H_2O_2 was still solid (Fig. 5 (c)). Which shows that the C-CS-Cys hydrogel had a redox response, breaking the disulfide bonds in the hydrogel in ROS environment produced by H_2O_2. In this way, the crosslinking of the hydrogel was disconnected, and the hydrogel was disintegrated. Accordingly, it can be concluded that the C-CS-Cys hydrogel prepared in this paper had redox responsitivity.

Some of the nanoparticles prepared in this experiment were larger, so that they can be observed in the hydrogel pores by SEM, as Fig. 5(e–f). It showed that the surface of the drug-loaded C-CS-Cys/PAM-BAC hydrogel had many protrusions, whose roughness was significantly higher than that of the corresponding hydrogel without drugs, which proved that the ACD-NPs-RvE1 was successfully loaded in the C-CS-Cys/PAM-BAC hydrogel. The Energy Dispersive Spectrometer (EDS) was used to analyze the element composition of the protrusion (Point A on Fig. 5(e)) and the smooth surface (Point B on Fig. 5(f)), and the results were shown in Table 2. The content of nitrogen at point A was 0, because ACD-NPs-RvE1 did not contain nitrogen, but the C-CS-Cys/PAM-BAC hydrogel represented by point B contained 1.9% nitrogen, which proved that the ACD-

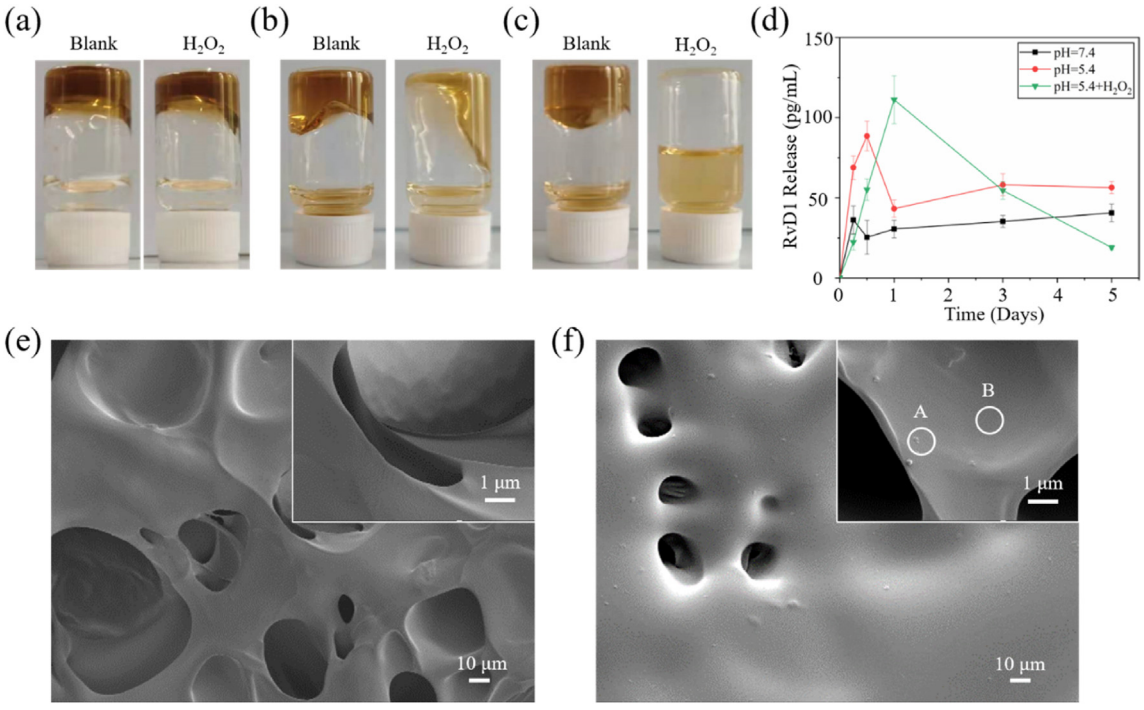

Fig. 5. C-CS-Cys hydrogels immersed in PBS or PBS with 5% H_2O_2 at (a) the first time, (b) 3 days, (c) 6 days. (d) Release curve of RvD1 loaded C-CS-Cys/PAM-BAC hydrogel. (e) SEM image of C-CS-Cys/PAM-BAC hydrogel without drug; and (f) SEM image of RvE1 loaded C-CS-Cys/PAM-BAC hydrogel.

Table 2
EDS element analysis on the surface of drug-loaded C-CS-Cys/PAM-BAC hydrogel.

Sample	C (%)	N (%)	O (%)
A	81.2	0	18.8
B	85.4	1.9	12.7

NPs-RvE1 were successfully loaded into C-CS-Cys/PAM- BAC hydrogel.

Fig. 5 (d) showed the release behavior of the ACD-NPs-RvD1 loaded C-CS-Cys/PAM-BAC hydrogel under various conditions. In the first 6 h, the RvD1 had a burst release from the C-CS-Cys/PAM-BAC hydrogel. The hydrogels were immersed in pH = 5.4 and in pH = 5.4 with 2 mM H_2O_2, and the drugs were still quickly released until 1 day. The hydrogel in pH = 5.4 with 2 mM H_2O_2 had the highest RvD1 release at the end of day 1. This confirmed that the ACD-NPs-RvD1 loaded C-CS-Cys/PAM-BAC hydrogel had an intelligent release characteristic of drugs, according to the changed of pH and ROS concentration. However, the release of RvD1 decreased after 1 days, which might cause by drugs exhaustion.

3.8. Cell growth on the ACD-NPs-RvE1 loaded C-CS-Cys/PAM-BAC hydrogels

The ACD-NPs-RvE1 loading to the C-CS-Cys/PAM-BAC hydrogels affected the proliferation of macrophages, as shown in Fig. 6(a–b). The proliferation of macrophages on the surface of blank hydrogels or hydrogels loaded with drug at various concentrations was low at 1 day, and the macrophages on each hydrogel proliferated significantly at 3 days with signs of aggregation on the samples. At day 5, compared with the blank hydrogel, the macrophage proliferation of the drug-loaded group was inhibited. This may be attributed to the anti-inflammatory effect of the slowly released drug.

The release of inflammatory factors TNF-α and IL-10 in macrophages cultured with different samples was shown in Fig. 6(c–d). At 1 day, macrophages cultured with hydrogels containing high concentrations of RvE1 released significantly more tumor necrosis factor-α (TNF-α) than other groups, when macrophages cultured with the inflammation regulator RvE1 released less interleukin 10 (IL-10) than those without drugs. On day 3, macrophages cultured with samples containing high RvE1 concentrations began to release more IL-10 than the blank hydrogel group. On day 5, the release of IL-10 in the three groups containing RvE1 for culturing macrophages exceeded the other two groups. This result indicated that RvE1 regulated the differentiation of macrophage phenotype to M_2 and promoted the secretion of anti-inflammatory factors, thereby playing anti-inflammatory effects [48,49].

Fig. 6 (e) showed the macrophages chemotaxis on the different samples. Macrophages can pass through the transwell under the influence of the sample. The result indicated that the ACD-NPs loaded C-CS-Cys/PAM-BAC hydrogels promoted chemotactic migration of macrophages. Hydrogel loaded 40 ng/mL RvE1 also promoted macrophage chemotaxis, but the chemotaxis decreased with increasing RvE1.

The results ACD-NPs-RvE1 loaded C-CS-Cys/PAM-BAC hydrogels affected the proliferation ability of L929 as shown in Fig. S7. At 1 day, it was weak that the proliferation ability of L929 cells on the surface of each group, and there was no significant change. And at 5 days, L929 cells on the surface of the drug-loaded and the ACD-NPs group was observed obvious proliferation, especially the C-CS-Cys/PAM-BAC hydrogel with 80 ng/mL RvE1 added. The reason of this result may be the effect of drug release.

In vitro biocompatibility test of the RvE1 loaded DN hydrogel showed good growth of both L929 cells and macrophages on the hydrogel. The proliferation of the two cell types was poor at 1 day, but the proliferation improved at 3–5 days.

3.9. ACD-NPs-RvE1 loaded DN hydrogel as wound dressing on the back of SD rats

A schematic diagram of the hydrogels placed on the back of rats to promote wound healing was shown in Fig. 7 (a). The closure of the skin wounds of SD rats indicated that C-CS-Cys/PAM-BAC hydrogel promoted the healing of the wounds. After adding ACD-NPs-RvE1, the wound healing was obviously promoted (Fig. 7 (b)). At 20 days, the wound was almost completely disappeared and covered by new hair. The 20-day hematoxylin-eosin staining (HE staining) of the wound (Fig. 7 (c)) clearly shows the healing condition. The PBS group had larger immature tissue with a diameter of about 6000 μm, and the blank hydrogel group and the ACD-NPs group were slightly smaller than the PBS group with a diameter of about 4000 μm. In the group with RvE1, the area of mature tissue was significantly increased, and the wound diameter was 2000–2500 μm. This further proved that both RvE1 and the hydrogel promoted wound healing.

The collagen content was another indicator of successful wound healing. Fig. 7 (d) showed the Masson stain images of the wound at 20 days. The collagen in the tissue in the picture appears blue. It can be seen that the blue of the healed tissue was more intense, and the blue of the non-healed wound was lighter. These results indicated that the ACD-NPs-RvE1 loaded C-CS-Cys/PAM-BAC hydrogels had the best healing effect on wounds.

The number of new blood vessels on the back of SD rats was shown in Fig. 7 (e). The number of new blood vessels formation indicated the degree of wound repair. Combined with the Fig. 7 (c), the 120 ng/mL RvE1 loaded hydrogel induced the highest number of new blood vessels compared with other groups, which proved the RvE1 loaded wounds dressing promoted microangiogenesis and provided more nutrients to facilitate wound repair.

4. Discussion

In this work, we reported a double network (DN) hydrogels wound dressing, which had an enhanced mechanical properties and good biocompatibility. Also, we loaded the RvE1 in the DN hydrogels with ACD-NPs. In this way, the DN hydrogels wound dressing intelligent released the RvE1. The RvE1 could regulate the differentiation of macrophages to M2 phenotype, and released the IL-10 to promote tissue regeneration, in low pH and high ROS environment.

The DN hydrogels, obtained by incorporating polyacrylamide (PAM) into catechol chitosan (C-CS) hydrogels, significantly increased the mechanical properties of the hydrogels. That result was the same as the DN hydrogel prepared by interpenetration of a flexible and rigid network [14,50,51]. Natural macromolecular chitosan as the basic hydrogel successfully enhanced the mechanical properties for general requirements as wound dressing; it did hardly tear or drop off at daily activities [52,53]. In this work, the stronger mechanical properties of DN hydrogel might caused by the addition of PAM, or the more intermolecular forces between the two hydrogel networks, which non-covalent force dissipated energy during the deformation of the hydrogel [54]. For the cross-linking method of hydrogel, the results of XPS was proved that Cys was used as the cross-linking agent of C-CS, through Michael addition or Schiff base reaction between amino group and catechol quinone and accelerate the gelation speed of the hydrogel.

The disulfide bonds of Cys in the hydrogel network made the hydrogel ROS responsive [55–57]. For the two crosslinking agents (BAC and MBA) in the PAM network, the BAC containing disulfide bonds can also add more disulfide bonds in the DN hydrogel. Moreover, the disulfide bonds in BAC and Cys can have a dynamic exchange reaction, which enhanced the interaction between the two hydrogel networks. In addition, compared with the C-CS hydrogel, the swelling degree of the DN

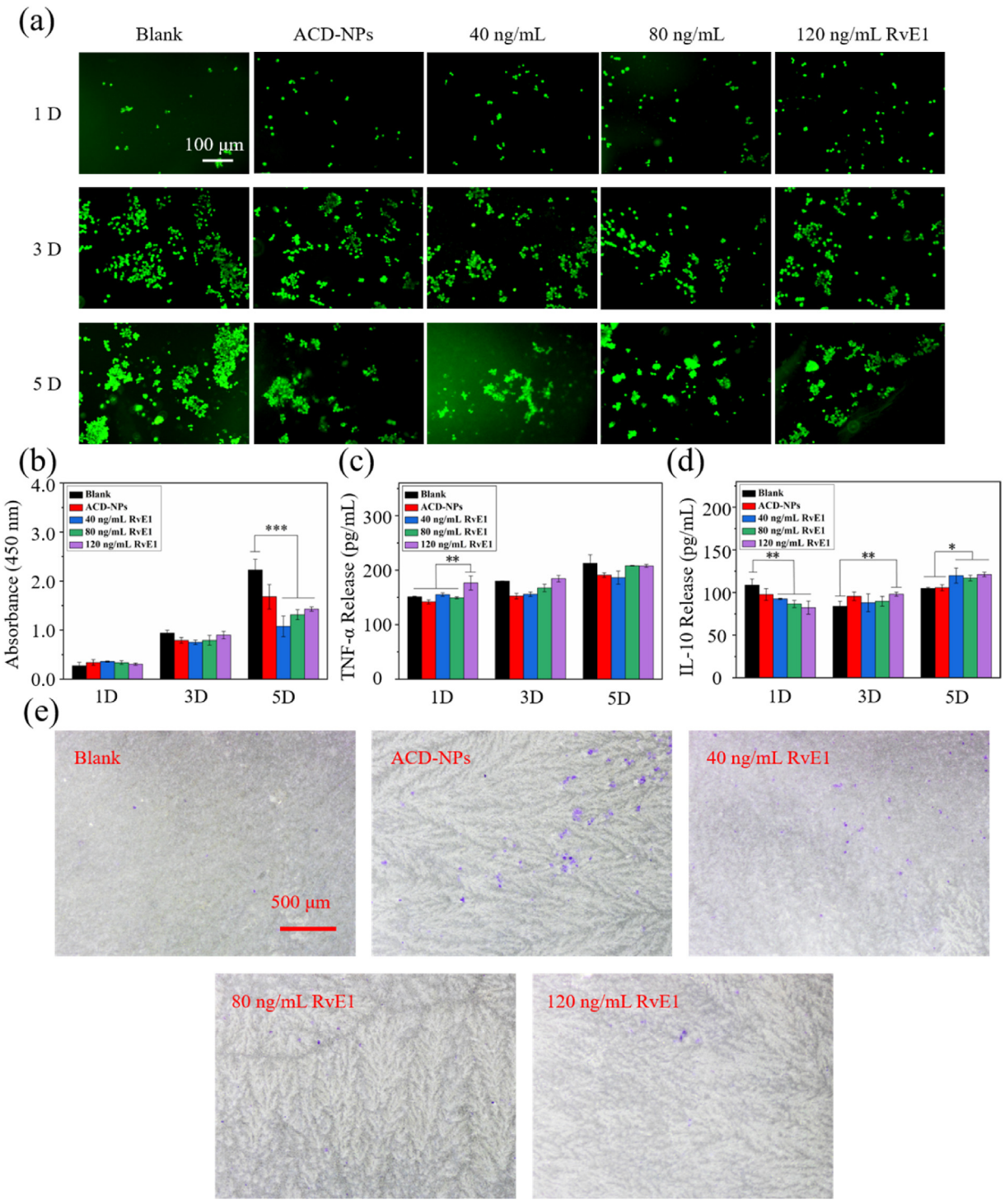

Fig. 6. (a) Fluorescence images of Acridine Orange (AO) stained macrophages on the surface of different hydrogel samples after 1, 3, 5 days. (b) CCK-8 analysis of the viability of macrophages on the surface of the different hydrogel samples at 1, 3, 5 days. (c) Release of TNF-α and (d) IL-10 from macrophages on different samples. (e) Macrophages chemotaxis behavior tested by transwell on different samples. (n = 3, *p < 0.05, **p < 0.01, ***p < 0.001). (For interpretation of the references to colour in this figure legend, the reader is referred to the Web version of this article.)

hydrogel prepared in this study greatly increased and the gels required more time to reach the swelling equilibrium. This was attributed to the hydrophilic property of PAM in the hydrogel system, and the cross-linking degree of the DN hydrogel with different crosslinking agents also influenced the swelling performance. Han et al. also used dopamine-composite chitosan and PAM to prepare hydrogels, which reached swelling equilibrium at 5 h, with mass swelling rates of 15.8 [58]. From another point of view, this also showed that the hydrogel formed by C-CS also enhanced the swelling performance of the DN hydrogel, which can make the DN hydrogel used as a wound dressing to absorb the exudate from the wound site [59].

The link of catechol groups into the hydrogels was an important way to enhance the wound healing capacity of the hydrogel wound dressings. The catechol groups enhanced the tissue and cell adhesion of the hydrogels, promoting wound healing [60,61]. Lu et al. used a catechol group to modify a hydrogel wound dressing, similar to the DN hydrogel

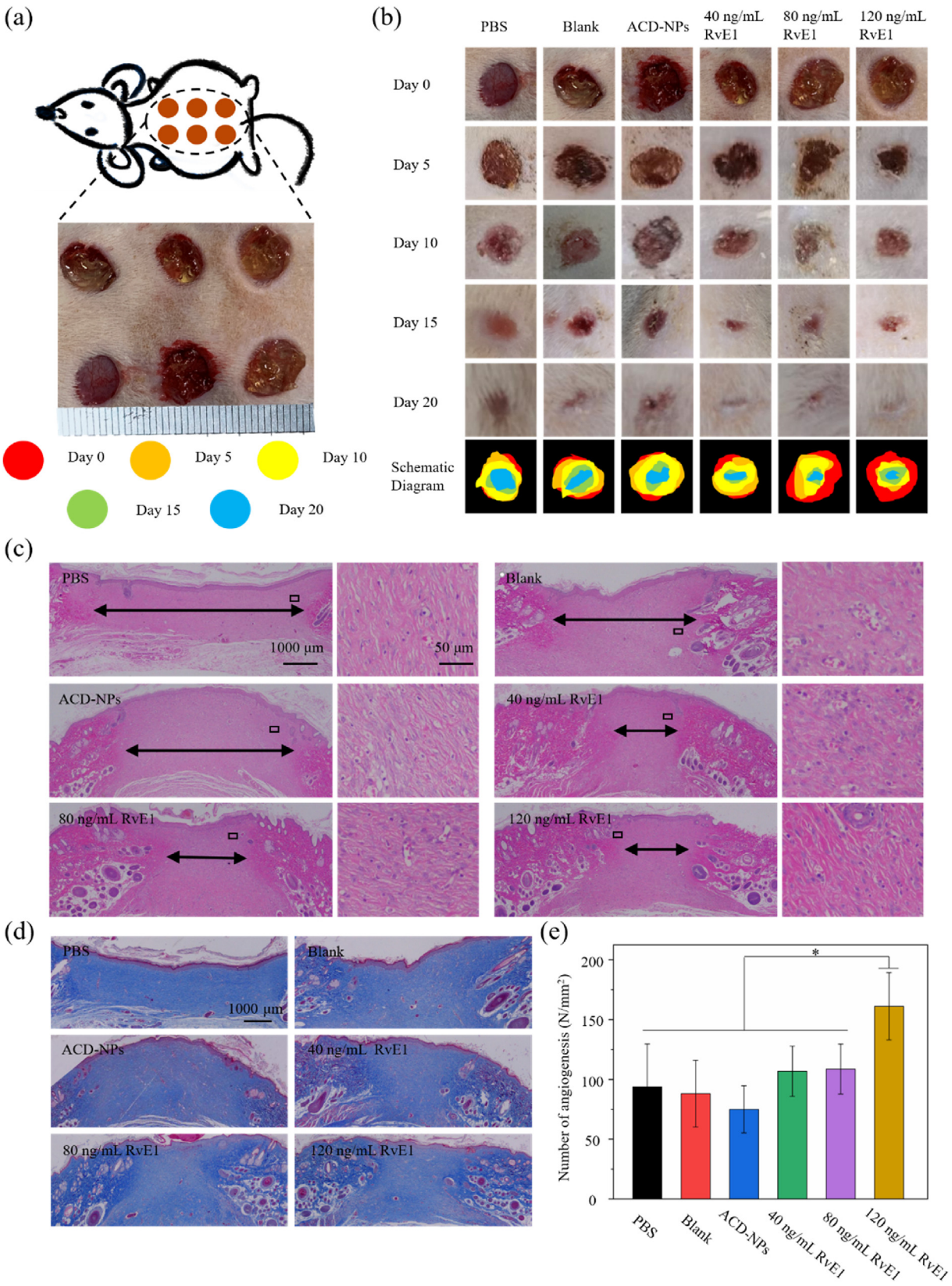

Fig. 7. (a) Schematic diagram of hydrogel wound dressing used for acute dermal wounds in the back of SD rats. (b) Photographs of DN hydrogel wound dressings promoting back wound healing in SD rats at 0, 5, 10, 15, and 20 days. (c) HE stain of wounds healed at 20 days. (d) Masson staining of wounds healed at 20 days. (e) The number of new blood vessels in the back of SD rats at 20 days. ($n = 5$, Pic $= 6$, $^*p < 0.05$).

of this study. This modification induced a significant promotion on the repair of rat back wounds [21], which was explained as the catechol group not only promotes cell adhesion and gathers in wounds, which could promote the revascularization, but also has a strong interaction with tissues [62].

The wound site was usually accompanied by inflammatory reactions, especially hard-to-heal wounds. The long-term chronic inflammation hindered the development of the wound to the proliferative phase and affects the repair processes of the wound.

Localized inflammation was usually characterized by the presence of many white blood cells, such as neutrophils and macrophages [63]. Macrophages were the one of main cells of inflammation, and can have different shapes and functions under various conditions. Before differentiation, macrophages usually existed in the form M_0. M_1 macrophages were generally activated through interferon-γ (IFN-γ) or lipopolysaccharide (LPS); they mainly secreted pro-inflammatory factors in the inflammatory reaction, such as TNF-α, IL-1. M_2 macrophages were activated by Th-2 cytokines and can be differentiated from M_0 macrophages or M_1 macrophages. Their primary function was the expression of anti-inflammatory factors, such as IL-10 and IL-4, which promoted tissue repair [64]. Vasconcelos et al. incorporated RvD1 (Derivatives of RvE1) into a 3D chitosan scaffold and found that it reduced the recruitment of inflammatory cells and promoted the conversion of macrophages to the M_2 phenotype [65]. In the hydrogel prepared in this study, the inflammation regulator factor RvE1 inhibited the proliferation of macrophages and inhibited the release of TNF-α, due to the phenotypic differentiation of macrophages, thereby suppressing inflammation and promoting neovascularization.

5. Conclusion

In this study, we designed a double-response drug delivery system, which can release the RvE1, one of the SPMs. This drug-carrying system used natural macromolecular CS with good biocompatibility as the first hydrogel network, and used PAM and cross-linking methods with or without disulfide bonds to make DN hydrogel, ACD was loaded to prepare responsive NPs, which can intelligently release drugs in the low pH and high ROS environment of inflammation. In addition, the swelling and mechanical properties of the DN hydrogel were significantly enhanced, compared with C-CS or C-CS-Cys hydrogels. The presence of catechol groups can be beneficial to cell adhesion which was conducive to cell proliferation. RvE1 can regulate wound inflammation and promote the expression of IL-10, which was beneficial to wound repair and healing. The design of this drug-carrying system has the advantages of potentially improving the difficult-to-control release of hydrogel drug release systems and the difficulty of loading hydrophobic drugs, and also provides a potential method for inflammation regulation in promoting wound healing, especially the healing of chronic wounds.

Credit author statement

Bingyang Lu: Investigation, Conceptualization, Visualization, Writing – original draft. **Xiao Han:** Investigation, Writing – original draft. **Dan Zou:** Investigation. **Xiao Luo:** Investigation, **Li Liu:** Investigation, **Jingyue Wang:** Investigation. **Manfred F. Maitz:** Visualization, Writing – review & editing. **Ping Yang:** Supervision. **Nan Huang:** Supervision. **Ansha Zhao*:** Supervision, Conceptualization, Visualization, Writing – review & editing.

Declaration of competing interest

The authors declare that they have no known competing financial interests or personal relationships that could have appeared to influence the work reported in this paper.

Acknowledgments

This work was supported by the National Natural Science Foundation of China (NSFC 81771988), and Department of Science and Technology of Sichuan Province (No. 2020YFH0025).

Appendix A. Supplementary data

Supplementary data to this article can be found online at https://doi.org/10.1016/j.mtbio.2022.100392.

References

[1] S. Sharifi, M.J. Hajipour, L. Gould, M. Mahmoudi, Nanomedicine in healing chronic wounds: opportunities and challenges, Mol. Pharm. 18 (2) (2021) 550–575, https://doi.org/10.1021/acs.molpharmaceut.0c00346.
[2] W.G. Liu, M. Wang, W. Cheng, W. Niu, M. Chen, M. Luo, C.X. Xie, T.T. Leng, L. Zhang, B. Lei, Bioactive antiinflammatory antibacterial hemostatic citrate-based dressing with macrophage polarization regulation for accelerating wound healing and hair follicle neogenesis, Bioact. Mater. 6 (3) (2021) 721–728, https://doi.org/10.1016/j.bioactmat.2020.09.008.
[3] G.D. Winter, Formation of the scab and the rate of epithelization of superficial wounds in the skin of the young domestic pig, Nature 193 (1962) 293–294, https://doi.org/10.1038/193293a0.
[4] Z.M. Li, Z.D. Chen, H.Z. Chen, K.B. Chen, W. Tao, X.K. Ouyang, L. Mei, X.W. Zeng, Polyphenol-based hydrogels: pyramid evolution from crosslinked structures to biomedical applications and the reverse design, Bioact. Mater. 17 (2022) 49–70, https://doi.org/10.1016/j.bioactmat.2022.01.038.
[5] X.Y. Liu, J. Liu, S.T. Lin, X.H. Zhao, Hydrogel machines, Mater. Today 36 (2020) 102–124, https://doi.org/10.1016/j.mattod.2019.12.026.
[6] N. Asadi, H. Pazoki-Toroudi, A.R. Del Bakhshayesh, A. Akbarzadeh, S. Davaran, N. Annabi, Multifunctional hydrogels for wound healing: special focus on biomacromolecular based hydrogels, Int. J. Biol. Macromol. 170 (2021) 728–750, https://doi.org/10.1016/j.ijbiomac.2020.12.202.
[7] S. Rashki, K. Asgarpour, H. Tarrahimofrad, M. Hashemipour, M.S. Ebrahimi, H. Fathizadeh, A. Khorshidi, H. Khan, Z. Marzhoseyni, M. Salavati-Niasari, H. Mirzaei, Chitosan-based nanoparticles against bacterial infections, Carbohydr. Polym. 251 (2021), 117108, https://doi.org/10.1016/j.carbpol.2020.117108.
[8] H. Hamedi, S. Moradi, S.M. Hudson, A.E. Tonelli, Chitosan based hydrogels and their applications for drug delivery in wound dressings: a review, Carbohydr. Polym. 199 (2018) 445–460, https://doi.org/10.1016/j.carbpol.2018.06.114.
[9] P.P. Feng, Y. Luo, C.H. Ke, H.F. Qiu, W. Wang, Y.B. Zhu, R.X. Hou, L. Xu, S.Z. Wu, Chitosan-based functional materials for skin wound repair: mechanisms and applications, Front. Bioeng. Biotechnol. 9 (2021), 650598, https://doi.org/10.3389/fbioe.2021.650598.
[10] Y. Chen, L. Huang, X. Dai, Q. Tian, M. Yu, M. Agheb, H.N. Chan, E. Poon, Z.H. Guo, K.R. Boheler, H.K. Wu, Facile formation of a microporous chitosan hydrogel based on self-crosslinking, J. Mater. Chem. B 5 (47) (2017) 9291–9299, https://doi.org/10.1039/c7tb02736b.
[11] K. Kiene, F. Porta, B. Topacogullari, P. Detampel, J. Huwyler, Self-assembling chitosan hydrogel: a drug-delivery device enabling the sustained release of proteins, J. Appl. Polym. Sci. 135 (1) (2018), 45638, https://doi.org/10.1002/app.45638.
[12] M.C.G. Pella, M.K. Lima-Tenorio, E.T.T. Neto, M.R. Guilherme, E.C. Muniz, A.F. Rubira, Chitosan-based hydrogels: from preparation to biomedical applications, Carbohydr. Polym. 196 (2018) 233–245, https://doi.org/10.1016/j.carbpol.2018.05.033.
[13] J.P. Gong, Y. Katsuyama, T. Kurokawa, Y. Osada, Double-network hydrogels with extremely high mechanical strength, Adv. Mater. 15 (14) (2003) 1155–1158, https://doi.org/10.1002/adma.200304907.
[14] X.W. Xu, V.V. Jerca, R. Hoogenboom, Bioinspired double network hydrogels: from covalent double network hydrogels via hybrid double network hydrogels to physical double network hydrogels, Mater. Horiz. 8 (4) (2021) 1173–1188, https://doi.org/10.1039/d0mh01514h.
[15] H. Lee, S.M. Dellatore, W.M. Miller, P.B. Messersmith, Mussel-inspired surface chemistry for multifunctional coatings, Science 318 (5849) (2007) 426–430, https://doi.org/10.1126/science.1147241.
[16] W. Zhang, R.X. Wang, Z.M. Sun, X.W. Zhu, Q. Zhao, T.F. Zhang, A. Cholewinski, F. Yang, B.X. Zhao, R. Pinnaratip, P.K. Forooshani, B.P. Lee, Catechol-functionalized hydrogels: biomimetic design, adhesion mechanism, and biomedical applications, Chem. Soc. Rev. 49 (2) (2020) 433–464, https://doi.org/10.1039/c9cs00285e.
[17] J. Saiz-Poseu, J. Mancebo-Aracil, F. Nador, F. Busque, D. Ruiz-Molina, The chemistry behind catechol-based adhesion, Angew. Chem., Int. Ed. 58 (3) (2019) 696–714, https://doi.org/10.1002/anie.201801063.
[18] B. Zhang, Y. Qin, L. Yang, Y. Wu, N. Chen, M. Li, Y. Li, H. Wan, D. Fu, R. Luo, L. Yuan, Y. Wang, A polyphenol-network-mediated coating modulates inflammation and vascular healing on vascular stents, ACS Nano 16 (2022) 6585–6597, https://doi.org/10.1021/acsnano.2c00642.
[19] X.M. Fan, Y. Fang, W.K. Zhou, L.Y. Yan, Y.H. Xu, H. Zhu, H.Q. Liu, Mussel foot protein inspired tough tissue-selective underwater adhesive hydrogel, Mater. Horiz. 8 (3) (2021) 997–1007, https://doi.org/10.1039/d0mh01231a.
[20] Z.F. Yang, R.K. Huang, B.N. Zheng, W.T. Guo, C.K. Li, W.Y. He, Y.G. Wei, Y. Du, H.M. Wang, D.C. Wu, H. Wang, Highly stretchable, adhesive, biocompatible, and

antibacterial hydrogel dressings for wound healing, Adv. Sci. 8 (8) (2021), 2003627, https://doi.org/10.1002/advs.202003627.
[21] D.L. Gan, T. Xu, W.S. Xing, X. Ge, L.M. Fang, K.F. Wang, F.Z. Ren, X. Lu, Mussel-inspired contact-active antibacterial hydrogel with high cell affinity, toughness, and recoverability, Adv. Funct. Mater. 29 (1) (2019), 1805964, https://doi.org/10.1002/adfm.201805964.
[22] D.L. Gan, W.S. Xing, L.L. Jiang, J. Fang, C.C. Zhao, F.Z. Ren, L.M. Fang, K.F. Wang, X. Lu, Plant-inspired adhesive and tough hydrogel based on Ag-Lignin nanoparticles-triggered dynamic redox catechol chemistry, Nat. Commun. 10 (2019) 1487, https://doi.org/10.1038/s41467-019-09351-2.
[23] S. Bernhard, M.W. Tibbitt, Supramolecular engineering of hydrogels for drug delivery, Adv. Drug Deliv. Rev. 171 (2021) 240–256, https://doi.org/10.1016/j.addr.2021.02.002.
[24] Y. Lu, A.A. Aimetti, R. Langer, Z. Gu, Bioresponsive materials, Nat. Rev. Mater. 2 (1) (2017), 16075, https://doi.org/10.1038/natrevmats.2016.75.
[25] X. Fu, L. Hosta-Rigau, R. Chandrawati, J.W. Cui, Multi-stimuli-responsive polymer particles, films, and hydrogels for drug delivery, Chem 4 (9) (2018) 2084–2107, https://doi.org/10.1016/j.chempr.2018.07.002.
[26] M.F. Maitz, U. Freudenberg, M.V. Tsurkan, M. Fischer, T. Beyrich, C. Werner, Bio-responsive polymer hydrogels homeostatically regulate blood coagulation, Nat. Commun. 4 (2013) 2168, https://doi.org/10.1038/ncomms3168.
[27] M.F. Maitz, J. Zitzmann, J. Hanke, C. Renneberg, M.V. Tsurkan, C. Sperling, U. Freudenberg, C. Werner, Adaptive release of heparin from anticoagulant hydrogels triggered by different blood coagulation factors, Biomaterials 135 (2017) 53–61, https://doi.org/10.1016/j.biomaterials.2017.04.044.
[28] F.H. Meng, W.E. Hennink, Z. Zhong, Reduction-sensitive polymers and bioconjugates for biomedical applications, Biomaterials 30 (12) (2009) 2180–2198, https://doi.org/10.1016/j.biomaterials.2009.01.026.
[29] K. Miyata, Y. Kakizawa, N. Nishiyama, A. Harada, Y. Yamasaki, H. Koyama, K. Kataoka, Block catiomer polyplexes with regulated densities of charge and disulfide cross-linking directed to enhance gene expression, J. Am. Chem. Soc. 126 (8) (2004) 2355–2361, https://doi.org/10.1021/ja0379666.
[30] N. Murthy, Y.X. Thng, S. Schuck, M.C. Xu, J.M.J. Frechet, A novel strategy for encapsulation and release of proteins: hydrogels and microgels with acid-labile acetal cross-linkers, J. Am. Chem. Soc. 124 (42) (2002) 12398–12399, https://doi.org/10.1021/ja026925r.
[31] E.M. Bachelder, T.T. Beaudette, K.E. Broaders, J. Dashe, J.M.J. Frechet, Acetal-derivatized dextran: an acid-responsive biodegradable material for therapeutic applications, J. Am. Chem. Soc. 130 (32) (2008) 10494–10495, https://doi.org/10.1021/ja803947s.
[32] C.Y. Gong, Q.J. Wu, Y.J. Wang, D.D. Zhang, F. Luo, X. Zhao, Y.Q. Wei, Z.Y. Qian, A biodegradable hydrogel system containing curcumin encapsulated in micelles for cutaneous wound healing, Biomaterials 34 (27) (2013) 6377–6387, https://doi.org/10.1016/j.biomaterials.2013.05.005.
[33] J. Gan, Y. Dou, Y. Li, Z. Wang, L. Wang, S. Liu, Q. Li, H. Yu, C. Liu, C. Han, Z. Huang, J. Zhang, C. Wang, L. Dong, Producing anti-inflammatory macrophages by nanoparticle-triggered clustering of mannose receptors, Biomaterials 178 (2018) 95–108, https://doi.org/10.1016/j.biomaterials.2018.06.015.
[34] R.L. Zhao, H.L.N. Liang, E. Clarke, C. Jackson, M.L. Xue, Inflammation in chronic wounds, Int. J. Mol. Sci. 17 (12) (2016) 2085, https://doi.org/10.3390/ijms17122085.
[35] J. Huang, Y. Jiang, Y. Liu, Y. Ren, Z. Xu, Z. Li, Y. Zhao, X. Wu, J. Ren, Marine-inspired molecular mimicry generates a drug-free, but immunogenic hydrogel adhesive protecting surgical anastomosis, Bioact. Mater. 6 (3) (2021) 770–782, https://doi.org/10.1016/j.bioactmat.2020.09.010.
[36] C.N. Serhan, Pro-resolving lipid mediators are leads for resolution physiology, Nature 510 (7503) (2014) 92–101, https://doi.org/10.1038/nature13479.
[37] M. Back, A. Yurdagul, I. Tabas, K. Oorni, P.T. Kovanen, Inflammation and its resolution in atherosclerosis: mediators and therapeutic opportunities, Nat. Rev. Cardiol. 16 (7) (2019) 389–406, https://doi.org/10.1038/s41569-019-0169-2.
[38] J. Dalli, C.N. Serhan, Pro-resolving mediators in regulating and conferring macrophage function, Front. Immunol. 8 (2017) 1400, https://doi.org/10.3389/fimmu.2017.01400.
[39] M. Rodrigues, N. Kosaric, C.A. Bonham, G.C. Gurtner, Wound healing: a cellular perspective, Physiol. Rev. 99 (1) (2019) 665–706, https://doi.org/10.1152/physrev.00067.2017.
[40] X. Zhao, Y.P. Liang, Y. Huang, J.H. He, Y. Han, B.L. Guo, Physical double-network hydrogel adhesives with rapid shape adaptability, fast self-healing, antioxidant and NIR/pH stimulus-responsiveness for multidrug-resistant bacterial infection and removable wound dressing, Adv. Funct. Mater. 30 (17) (2020), 1910748, https://doi.org/10.1002/adfm.201910748.
[41] B.Y. Lu, D. Luo, A.S. Zhao, H.H. Wang, Y.C. Zhao, M.F. Maitz, P. Yang, N. Huang, pH responsive chitosan and hyaluronic acid layer by layer film for drug delivery applications, Prog. Org. Coating 135 (2019) 240–247, https://doi.org/10.1016/j.porgcoat.2019.06.012.
[42] R.J. Zhang, R.F. Liu, C. Liu, L.N. Pan, Y.T. Qi, J. Cheng, J.W. Guo, Y. Jia, J. Ding, J.X. Zhang, H.Y. Hu, A pH/ROS dual-responsive and targeting nanotherapy for vascular inflammatory diseases, Biomaterials 230 (2020), 119605, https://doi.org/10.1016/j.biomaterials.2019.119605.
[43] K. Kim, K. Kim, J.H. Ryu, H. Lee, Chitosan-catechol: a polymer with long-lasting mucoadhesive properties, Biomaterials 52 (2015) 161–170, https://doi.org/10.1016/j.biomaterials.2015.02.010.
[44] J.M. Zhang, X.Y. Tao, J.W. Liu, D.Z. Wei, Y.H. Ren, Fe3+-induced bioinspired chitosan hydrogels for the sustained and controlled release of doxorubicin, RSC Adv. 6 (53) (2016) 47940–47947, https://doi.org/10.1039/c6ra07369g.
[45] S.B. Ji, W. Cao, Y. Yu, H.P. Xu, Dynamic diselenide bonds: exchange reaction induced by visible light without catalysis, Angew. Chem., Int. Ed. 53 (26) (2014) 6781–6785, https://doi.org/10.1002/anie.201403442.
[46] R.J. Wojtecki, M.A. Meador, S.J. Rowan, Using the dynamic bond to access macroscopically responsive structurally dynamic polymers, Nat. Mater. 10 (1) (2011) 14–27, https://doi.org/10.1038/Nmat2891.
[47] J.X. Zhang, Y. Jia, X.D. Li, Y.Q. Hu, X.H. Li, Facile engineering of biocompatible materials with pH-modulated degradability, Adv. Mater. 23 (27) (2011) 3035–3040, https://doi.org/10.1002/adma.201100679.
[48] J.C. Gensel, B. Zhang, Macrophage activation and its role in repair and pathology after spinal cord injury, Brain Res. 1619 (2015) 1–11, https://doi.org/10.1016/j.brainres.2014.12.045.
[49] A. Shapouri-Moghaddam, S. Mohammadian, H. Vazini, M. Taghadosi, S.A. Esmaeili, F. Mardani, B. Seifi, A. Mohammadi, J.T. Afshari, A. Sahebkar, Macrophage plasticity, polarization, and function in health and disease, J. Cell. Physiol. 233 (9) (2018) 6425–6440, https://doi.org/10.1002/jcp.26429.
[50] J.P. Gong, Why are double network hydrogels so tough? Soft Matter 6 (12) (2010) 2583–2590, https://doi.org/10.1039/b924290b.
[51] Y.Y. Yang, X. Wang, F. Yang, L.N. Wang, D.C. Wu, Highly elastic and ultratough hybrid Ionic-covalent hydrogels with tunable structures and mechanics, Adv. Mater. 30 (18) (2018), 1707071, https://doi.org/10.1002/adma.201707071.
[52] E.A. Kamoun, E.R.S. Kenawy, X. Chen, A review on polymeric hydrogel membranes for wound dressing applications: PVA-based hydrogel dressings, J. Adv. Res. 8 (3) (2017) 217–233, https://doi.org/10.1016/j.jare.2017.01.005.
[53] E.A. Kamoun, X. Chen, M.S.M. Eldin, E.R.S. Kenawy, Crosslinked poly(vinyl alcohol) hydrogels for wound dressing applications: a review of remarkably blended polymers, Arab. J. Chem. 8 (1) (2015) 1–14, https://doi.org/10.1016/j.arabjc.2014.07.005.
[54] L. Han, L.W. Yan, K.F. Wang, L.M. Fang, H.P. Zhang, Y.H. Tang, Y.H. Ding, L.T. Weng, J.L. Xu, J. Weng, Y.J. Liu, F.Z. Ren, X. Lu, Tough, self-healable and tissue-adhesive hydrogel with tunable multifunctionality, NPG Asia Mater. 9 (2017) e372, https://doi.org/10.1038/am.2017.33.
[55] J. Liang, B. Liu, ROS-responsive drug delivery systems, Bioeng. Transl. Med. 1 (3) (2016) 239–251, https://doi.org/10.1002/btm2.10014.
[56] K. Dong, C.R. Yang, Y. Yan, P.C. Wang, Y. Sun, K. Wang, T.L. Lu, Q. Chen, Y.N. Zhang, J.F. Xing, Y.L. Dong, Investigation of the intracellular oxidative stress amplification, safety and anti-tumor effect of a kind of novel redox-responsive micelle, J. Mater. Chem. B 6 (7) (2018) 1105–1117, https://doi.org/10.1039/c7tb02973j.
[57] K.C. Yan, A.C. Sedgwick, Y. Zang, G.R. Chen, X.P. He, J. Li, J. Yoon, T.D. James, Sensors, imaging agents, and theranostics to help understand and treat reactive oxygen species related diseases, Small Methods 3 (7) (2019), 1900013, https://doi.org/10.1002/smtd.201900013.
[58] L. Han, M.H. Wang, P.F. Li, D.L. Gan, L.W. Yan, J.L. Xu, K.F. Wang, L.M. Fang, C.W. Chan, H.P. Zhang, H.P. Yuan, X. Lu, Mussel-inspired tissue-adhesive hydrogel based on the polydopamine-chondroitin sulfate complex for growth-factor-free cartilage regeneration, ACS Appl. Mater. Interfaces 10 (33) (2018) 28015–28026, https://doi.org/10.1021/acsami.8b05314.
[59] J.D.C. Candido, N.A. Conceicao, A.P.D. Moreira, L.A. Calcada, L.S. Araujo, R.A. dos Santos, A. Middea, R. Luchese, E.R. Prudencio, R.N. Castro, G.B. McGuinness, R.N. Oliveira, Alginate hydrogels incorporating neomycin or propolis as potential dressings for diabetic ulcers: structure, swelling, and antimicrobial barrier properties, Polym, Adv. Met. Technol. 30 (10) (2019) 2623–2635, https://doi.org/10.1002/patA679.
[60] C.M. Xie, X. Wang, H. He, Y.H. Ding, X. Lu, Mussel-inspired hydrogels for self-adhesive bioelectronics, Adv. Funct. Mater. 30 (25) (2020), 1909954, https://doi.org/10.1002/adfm.201909954.
[61] J.H. Ryu, Y. Lee, W.H. Kong, T.G. Kim, T.G. Park, H. Lee, Catechol-functionalized chitosan/pluronic hydrogels for tissue adhesives and hemostatic materials, Biomacromolecules 12 (7) (2011) 2653–2659, https://doi.org/10.1021/bm200464x.
[62] R. Wang, J.Z. Li, W. Chen, T.T. Xu, S.F. Yun, Z. Xu, Z.Q. Xu, T. Sato, B. Chi, H. Xu, A biomimetic mussel-inspired epsilon-poly-L-iysine hydrogel with robust tissue-anchor and anti-Infection capacity, Adv. Funct. Mater. 27 (8) (2017), 1604894, https://doi.org/10.1002/adfm.201604894.
[63] M.J. Qian, X.C. Fang, X.D. Wang, Autophagy and inflammation, Clin. Transl. Med. 6 (1) (2017) 24, https://doi.org/10.1186/s40169-017-0154-5.
[64] K.L. Spiller, R.R. Anfang, K.J. Spiller, J. Ng, K.R. Nakazawa, J.W. Daulton, G. Vunjak-Noyakovic, The role of macrophage phenotype in vascularization of tissue engineering scaffolds, Biomaterials 35 (15) (2014) 4477–4488, https://doi.org/10.1016/j.biomaterials.2014.02.012.
[65] D.P. Vasconcelos, M. Costa, I.F. Amaral, M.A. Barbosa, A.P. Aguas, J.N. Barbosa, Development of an immunomodulatory biomaterial: using resolvin D1 to modulate inflammation, Biomaterials 53 (2015) 566–573, https://doi.org/10.1016/j.biomaterials.2015.02.120.